Synthesis of LFP by Fe-P alloy recovered from steelmaking slag
製鋼スラグの熱炭素還元で得た Fe-P 合金からの LFP 電池正極材原料 $FePO_4$ の製造

研究代表者　東北大学多元物質科学研究所　助教　岩間 崇之
共同研究者　東北大学多元物質科学研究所　教授　植田 滋
共同研究者　東北大学未来科学技術共同研究センター
シニアリサーチフェロー　佐々木 康

概要

今後、電気自動車(EV)の電池の正極材は多くが LFP になると考えられる。LFP は原料として安価な鉄やリンが豊富にあることを前提としているが、経済的に採掘可能なリン鉱石は 2030 年ころピークに達しその後は減少すると予測され、リン価格も上昇すると思われる。このため、リン産出国はリンの輸出規制を強化しており、リンの輸出が減ることはあっても増えることはない。よって現在、リンを全量輸入している日本では LFP 原料用のリンを新たに確保することは非常に困難となるため、輸入リンに代わるリン原料を早急に確保する必要がある。

日本はリン鉱石資源を持たないが国内には下水汚泥や製鋼スラグなどの 2 次リン資源がある。特に製鋼スラグには日本が輸入している総リン分に匹敵する約 30 万トンが含まれている。これまでの製鋼スラグからのリン回収研究は肥料用のリン回収を目的としていたため、鉄を分離し、リンのみを回収することが検討されてきた。 しかし、LFP 製造のりん回収を考えた場合、スラグ中の鉄とリンを同時に回収して LFP 原料の $FePO_4$ とするほうが合理的である。

この観点から、本研究は従来のアプローチとは全く異なり、製鋼スラグの熱炭素還元で発生したリンを同時に生成する還元鉄に可能な限り固溶させ、スラグ中のリンを Fe-P 合金として回収した後、その合金を酸溶解しその溶液の pH 調整により LFP 原料の $FePO_4$ を製造することを目的とし、所定の実験条件で $FePO_4$ の作成が可能である事を示した。

1. Introduction

Electric vehicles(EVs) have developed rapidly in recent years to address the CO_2 issue.[1,2] The global stock of EVs, including battery electric vehicles (BEV) and plug-in hybrid electric vehicles (PHEV), is expected to reach 220 million by 2030.[3] The rapid development of EVs relies on stable electrode materials. Lithium batteries are widely used in the EV industry.[4] Conventional lithium batteries include $LiMn_2O_4$ series, $LiCoO_2$ series, $Li(NiCoMn)O_2$ series and $Li(NiCoAl)O_2$ series.[2] These materials are widely used in the electric vehicle industry due to their high battery capacity. However, these series contain rare heavy metals, such as Mn, Co, and Ni. These metals are facing depletion and are soon difficult to obtain, making them expensive.[5–8] Furthermore, lithium cobalt oxide cells have a potential safety hazard due to their overcharging.[6] Therefore, there is a strong need for cathode materials made from inexpensive and stably available materials that do not contain these rare metals.

LFP attracts attention as a cathode electrode material to replace the rare metal-based ones, and already about 60% of cathode electrode material in China is LFP.[1,2] LFP as an electrode material has the advantages of low cost, high safety, non-toxic and recyclable.[7,9] The required iron source and phosphorus source are cheap raw materials for synthesising LFP.

With EV production increasing rapidly, a huge amount of LFP, or phosphorus will be required. It is predicted that the primary demand for phosphorus flow in the LFP production will reach 3Mt by 2050.[14] Although used LFP batteries can be used as raw materials for LFP production, because of their long service life, the current market for LFP batteries has not reached the point where used LFP batteries could meet the need for raw material for LFP production. This undoubtedly places great pressure on the source of raw materials for LFP production, especially on the utilisation and distribution of phosphorus sources.

To avoid this crisis with the limited resources of phosphate ores, we need to find new phosphorus resources. One is the recycling of spent LFP, but it will take several decades before the used LFP is put on the market.[11–13] An alternative approach is to use domestic secondary phosphorus resources until the spent LFP is put on the market. Waste ash, the incinerated sewage sludge and animal manure, is currently considered a promising secondary phosphorus resource.[14–17] At the same time, steelmaking slag has also attracted increasing attention recently.[18-22]

The steelmaking slag contains phosphorus, which originates from the iron ores and needs to be removed in the steel products to get rid of brittleness. The phosphorus content in the iron ore is greatly enriched in the steelmaking slag after the

dephosphorization treatment and exists as P_2O_5 at approximately 2 to 10 mass%. The content of phosphorus also restricts the usage of steelmaking slag. Once phosphorous is separated from steelmaking slags, the steelmaking slag can be reused in the sinter ore plant as well as in architectural engineering. Thus, many studies have been conducted to separate the phosphorus from the steelmaking slag.[18,21,23]

Previous researchers studied the acid leaching of steelmaking slag to enrich the phosphorus in the leachate and recycle it. Du et al. used hydrochloric acid to leach steelmaking slag with a controlled solution pH of 3. 81.6% of the phosphorus in the slag was dissolved, and the phosphorus was recovered as P_2O_5.[24] Iwama et al. used nitric acid for the leaching of steelmaking slag and pre-treated the slag in advance, thereby inhibiting the leaching of the impurity phase, which ultimately recycled 91% of the phosphorus in the slag.[21] As one of the recovery processes, phosphorous was captured as $FePO_4$ from slag leaching extract. Since $FePO_4$ is known to be the precursor material for producing LFP based on its olivine structure.[25,26]

Thus, considering LFP production, it is more rational to simultaneously recover iron and phosphorus from slag and use them as the LFP raw material $FePO_4$. From this perspective, this research has been carried out completely different from conventional approaches, aiming to dissolve as much phosphorus generated during the carbothermal reduction of steelmaking slag as possible into the reduced iron that is also produced at the same time, recover the phosphorus from the slag as an Fe-P alloy, and then dissolve the alloy in acid and adjust the pH of the solution to produce the LFP raw material $FePO_4$.

2. Synthesis of LFP by Fe-P alloy reduced from steelmaking slag

Due to the strong affinity between P and Fe, it was shown that P in steel slag can be directly enriched and recovered in the form of Fe-P alloys by carbothermal reduction.

To optimise P from steelmaking slag, in this study, the steelmaking slag is mixed with extra FeO. The Fe-P alloy will be used as a raw material to prepare LFP product via $FePO_4$ intermediate.

3. Experimental Methods

3.1 Preparation of samples

This study investigates the formation behavior of Fe-P alloy during the carbothermic reduction of steelmaking slag under different FeO ratios. Therefore, steelmaking slag was mixed with 10% and 20% FeO as experimental raw material. Specifically, additional FeO was 10% and 20% of the mass amount of steelmaking slag. The initial

slag, the samples with 10% and 20% FeO are labeled as Sample A, Sample B and Sample C. The specific compositions of the samples are shown in Table 1. Before mixing the steelmaking slag with FeO, the slag was ball-milled in order to destroy the mineral phase structure of the slag and become a glassy state with uniform element distribution, thus facilitating the reaction. The steelmaking slag was ball-milled at 300 revolutions per minute (rpm) for 4 hours. The milled steelmaking slag was then mixed with FeO to prepare samples B and C.

Samples A, B and C were mixed with carbon powder. The carbon powder was used as a reducing agent to reduce the iron oxides and phosphorus oxides in the samples at high temperatures. In order to make sure that all the iron oxides and phosphorus oxides were sufficiently reduced, an excess amount of carbon powder was used for the mixing. Due to the competitive relationship between the solubility of carbon and phosphorus in iron, the amount of carbon powder could not be too high, and finally, twice the carbon equivalent was selected for the experiment. The mixed samples were pressed into blocks of 1 cm diameter at a pressure of 200 mPa.

Table 1 The components of Sample A, B and C (mass %)

No.	CaO	SiO_2	T-Fe	FeO	Fe_2O_3	M-Fe	Additional FeO
Sample A	31.3	19.0	22.1	19.2	7.3	2.1	-
Sample B	28.5	17.3	27.9	17.5	6.6	1.9	9.1
Sample C	26.1	15.8	34.0	16.0	6.1	1.8	16.7
No.	Al_2O_3	MnO	MgO	P_2O_5	f-CaO	f-MgO	
Sample A	3.4	5.4	6.3	3.2	2.1	0.004	
Sample B	3.1	4.9	5.7	2.9	1.9	0.004	
Sample C	2.8	4.5	5.3	2.7	1.8	0.003	

3.2 Carbothermal reduction experiment

The samples were placed in an alumina crucible and placed in a vertical resistance

furnace, and Ar gas was introduced to conduct high-temperature experiments. According to previous studies, liquid iron and slag phase coexist at 1300℃, providing conditions for the carbothermic reduction reaction, so 1300℃ was used for the experiment.[22] The overall experimental flow and the heating program are shown in Figure 1 (d). The samples were placed in an Ar atmosphere, heated up to 1300℃, and held at the temperature for 5 hours. At the end of the holding period, the temperature was reduced at a rate of 3℃/min.

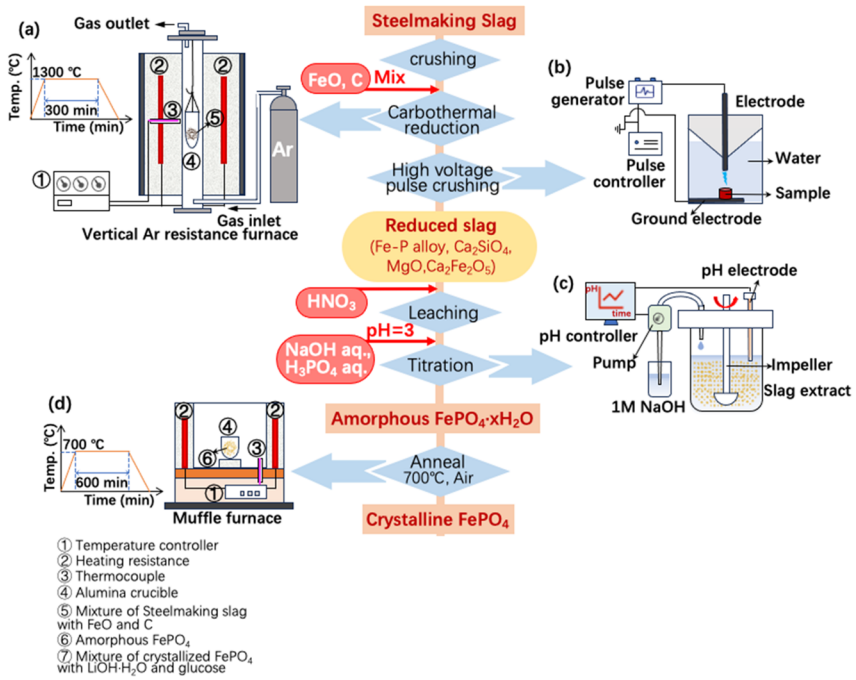

Figure 1 The experimental flow of synthesis on LFP using steelmaking slag through (a) the carbothermal reduction treatment of the slag, (b) the high voltage pulse crushing treatment of the slag, (c) pH adjustment for precipitation of $FePO_4$, (d) heating treatment of amorphous $FePO_4$

3.3 High voltage pulse selective crushing experiments

The samples after the carbothermal reduction reaction were crushed using a high voltage pulse selective crushing equipment for separating the produced Fe-P alloy from the slag phase. The separated Fe-P alloy will be easier for subsequent leaching experiments. The high voltage pulse selective crushing equipment is shown schematically in Figure 1 (b), which operates a high voltage pulse on the material, utilizing the difference in electrical conductivity between the different phases in the

material to crush and separate the sample.[27] The voltage value of 150kV, pulse frequency of 5hz, number of pulses of 300 times, and the distance between the electrode and the sample surface of 10mm were selected.

3.4 Synthesis of $FePO_4$ from Fe-P alloys

To synthesise $FePO_4$ from Fe-P alloy, it is necessary to first explore the experimental conditions suitable for precipitating $FePO_4$ from Fe-P alloy. The suitable pH and experimental parameters for $FePO_4$ precipitation were first explored using Fe_3P reagent. 0.1g Fe_3P reagent was leached in 60mL 1M HNO_3, and the leachate was treated for pH adjustment. The leachate was titrated using 1M NaOH solution, and the titration endpoints pH = 2 and 3 were chosen. As the NaOH titration proceeded, the solution was filtered when the pH of the solution reached the specified endpoint. To ensure the generation of LFP while avoiding the co-precipitation of $Fe(OH)_3$, H_3PO_4 was added to the solution to adjust the Fe/P ratio to 1:1. The precipitation was calcined in air at 700℃ for 10 hours and the heat-treated samples were subjected to XRD.

After determining the suitable precipitation conditions, the samples after high voltage pulse crushing were operated in the same way to obtain $FePO_4$. After $FePO_4$ was precipitated from the solution, it was placed in a muffle furnace for crystallisation (Figure 1 (d)).

3.5 Analysis

An X-ray diffraction measurement with a scan speed of 2°/min over a 2θ A range from 10 to 70° was used to check the crystallisation of the samples after the carbothermal reduction reaction. A scanning electron microscope (SEM) was used to observe the morphology of the samples before and after the high voltage pulse selective crushing experiment. An inductively coupled plasma atomic emission spectroscopy (ICP-AES) was used to analyse the concentration of each element in the samples. The standards with different concentration gradients of Fe, Ca, Si, Mg, Al, Mn and P were prepared, and the samples' content was obtained by comparing the test results with the standards. For preparing the solution used for ICP-AES analysis, the powder samples were dissolved in aqua regia.

4. Results and Discussion

4.1 Preparation of Fe-P alloys

The results of XRD of Samples A, B and C after carbothermal reduction at high temperature are shown in Figure 2.

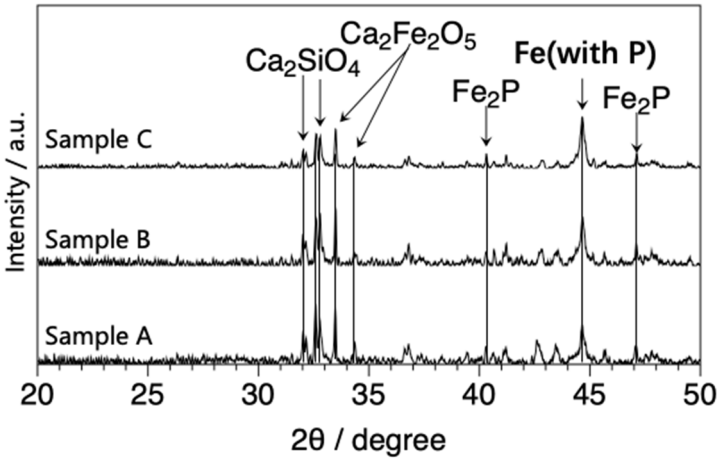

Figure 2　XRD results of the slag with 0~20% extra FeO after C reduction

The results show that the reduction products show Fe_2P as well as Fe peaks in addition to Ca_2SiO_4 and $Ca_2Fe_2O_5$. Compared with the standard card for Fe, the peaks for pure iron are 2theta=44.76°. However, the peaks in the XRD of Samples A, B and C are 2theta=44.65°, 44.68°, and 44.66°, respectively. This indicates that there is a penetration of P into the reduced iron, which leads to a shift in Fe peak in the XRD results.

From the Fe-P phase diagram shown in Figure 3,[22] it can be seen that a liquid phase region exists in the Fe-P alloy as the P content changes at 1300℃. As the liquid phase Fe-P alloy cools down from 1300℃, the Fe-P alloy will precipitate Fe_2P and Fe_3P products. Combined with the Fe_2P phase generated in the XRD results, it can be seen that the P content in the Fe-P alloy at this time is between 16% and 22%. It is shown that Fe can capture the P in the slag and form the Fe-P alloy directly through the reduction reaction.

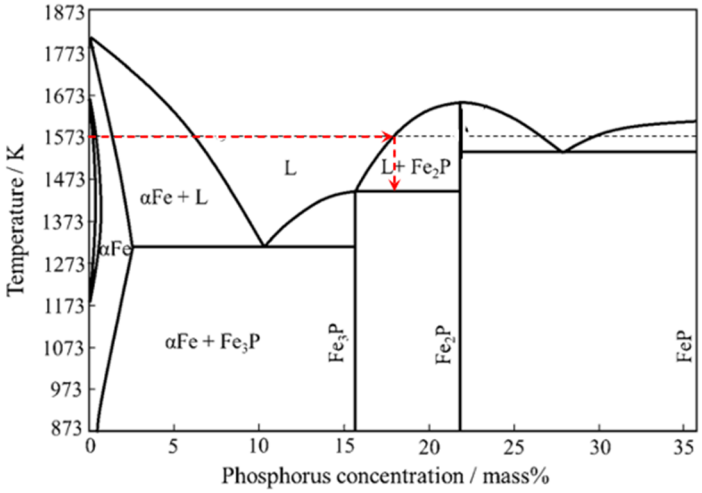

Figure 3　Fe-P phase diagram[22]

In order to further clarify the amount of P dissolved in the reduced Fe during the carbothermic reduction process, the samples were dissolved in aqua regia and then subjected to ICP analysis. The results of the Fe and P concentration change have been analysed and shown in the bar figures (Figure 4). The results show that the concentration content of the absorbed P element increases from Sample A to B, but remains constant from Sample B to C (Figure 4 (a)). The addition of FeO to the steelmaking slag captures more phosphorus, forming Fe-P alloys.

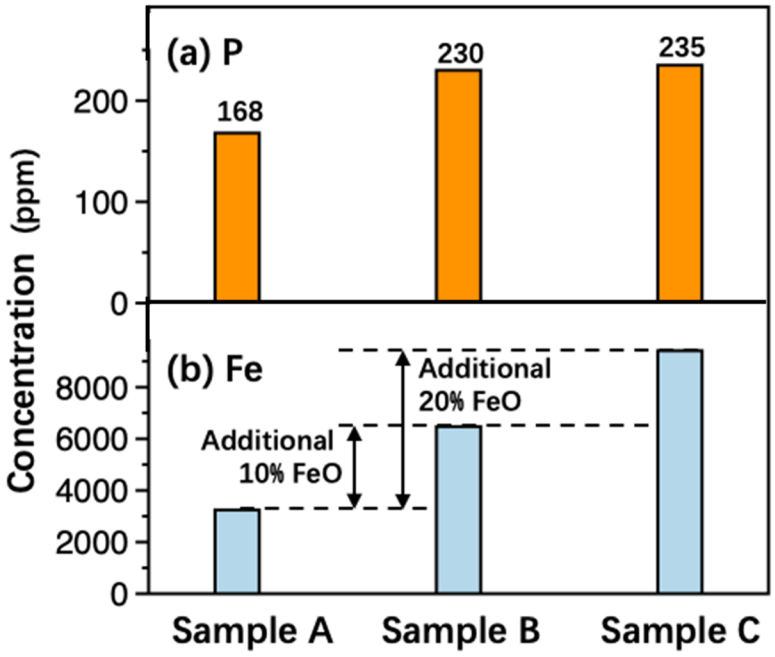

Figure 4　Concentration of Fe and P in Samples A, B and C after ICP analysis

The concentration of Fe and P of the reduced product was compared with the initial steelmaking slag to calculate the concentration flow of P from the slag to the Fe-P alloy, and the results showed that 61% of P in the steelmaking slag dissolved in the Fe-P alloy in Sample A, and this rate increases to 84% in Sample B and slightly changes to 87% in Sample C. That is, 10% and 20% additional FeO increase the P recovery ratio from initial slag by 37% and 43% through the carbothermic reduction method, respectively.

4.2 Synthesis of FePO4 from Fe-P alloys

Based on the thermodynamic evaluation, $FePO_4$ begins to precipitate when the pH = 1.5. A small amount $Fe(OH)_3$ precipitation also occurs when pH=3, so acid leaching of Fe-P alloys was attempted at pH=2 and 3 to obtain$FePO_4$.

The XRD results obtained at pH=2 and 3 are shown in Figure 5.

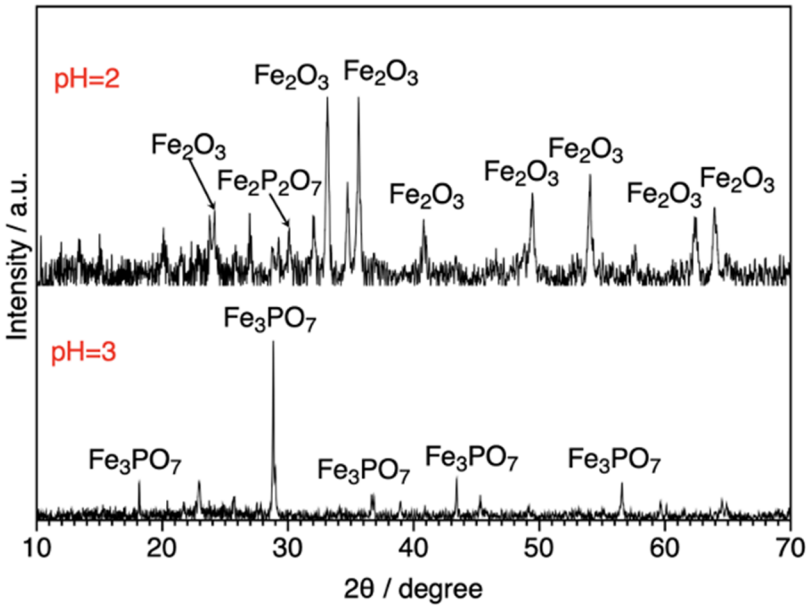

Figure 5　XRD results of the precipitation using Fe_3P reagents solution by pH controlled at 2 and 3

The suitable conditions for the process of precipitating $FePO_4$ were first explored using Fe_3P reagent. After dissolving Fe_3P in nitric acid (1M), the pH was adjusted to 2 and 3, respectively. The XRD results indicated that the final product obtained was Fe_3PO_7 when the pH of the solution was adjusted = 3.

When the pH of the solution was controlled to be 2, the XRD results showed that the precipitates were mainly Fe_2O_3, which also contained a small amount of iron phosphate ($Fe_2P_2O_7$). This shows that pH=2 is not a suitable pH for $FePO_4$ precipitation. At pH=2,

$Fe(OH)_3$ is preferentially precipitated. These results were obtained using Fe_3P.

To evaluate the effect of Fe/P, H_3PO_4 was added to the solution to ensure that Fe/P = 0.6 ~ 1.0.

Experiments were carried out using Sample C, which was first dissolved in nitric acid, and H_3PO_4 was added to the dissolved solution, first controlling the Fe/P ratio to be 1.0, and the precipitate was examined by XRD. The results show that when Fe/P=1.0, the precipitation still contained Fe_2O_3, with a complex iron phosphate ($Fe_4(PO_4)_2O$), indicating that, unlike the previous Fe^{3+} titration into the solution, the addition of H_3PO_4 still preferentially precipitates $Fe(OH)_3$ over $FePO_4$, and therefore requires an iron to phosphorus ratio of <1.

The additional H_3PO_4 was added to increase the Fe/P ratio in the solution to 0.6, and the XRD result (Figure 6) showed that the precipitate was $FePO_4$. Therefore, it is confirmed to produce $FePO_4$ from Fe-P alloys, the pH of the solution must be controlled at 3, and the Fe/P ratio should be controlled at 0.6.

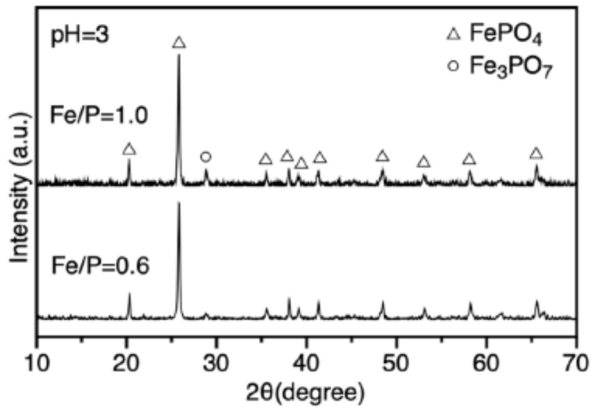

Figure 6　XRD results of precipitates when the pH of the extraction solution was 3, and the Fe/P ratio was 1.0 and 0.6

Initially, we had planned to consider carbothermal reduction using pellets with a two-phase structure in order to prevent the reduced phosphorus from escaping as a gas outside the pellets. However, we found that approximately 90% of the phosphorus was able to dissolve in the iron even without a two-phase structure, so we decided not to carry out carbothermal reduction using pellets with a two-phase structure.

5. Conclusions

To directly utilise the phosphorus and Fe in steelmaking slag to a greater extent, the carbothermal reduction experiment was carried out by dosing FeO in steelmaking slag, and the resulting Fe-P alloy was used as raw material to prepare the LFP product. The obtained results are summarised as follows:

(1) The phosphorus in the steelmaking slag can dissolve into the iron during the carbothermal reduction reaction and form Fe-P alloys. At the end of the reaction, 61% of the phosphorus in the steelmaking slag is captured by the Fe-P alloys.

(2) Carbothermicl reduction of steelmaking slag with additional FeO can increase the capture rate of phosphorus. The addition of 10% and 20% FeO increased the alloyed amount of P in the slag to 84% and 87%, respectively.

(3) For the production of $FePO_4$ from Fe-P alloys, after dissolving the Fe-P alloys in nitric acid solution, it is necessary to adjust the pH and Fe/P ratio of the solution to produce $FePO_4$ precipitation. pH should be controlled at 3, and the Fe/P ratio should be controlled at 0.6.

Aknowledgement

This research was supported by the JFE21 Foundation's FY2023 Technical Research Grant. We would like to express our gratitude to all involved parties.

References

(1) Li, X.; Wang, Z.; Zhang, L.; Sun, F.; Cui, D.; Hecht, C.; Figgener, J.; Sauer, D. U. Electric Vehicle Behavior Modeling and Applications in Vehicle-Grid Integration: An Overview. *Energy* **2023**, *268*, 126647. https://doi.org/10.1016/j.energy.2023.126647.

(2) Wang, W.; Wu, Y. An Overview of Recycling and Treatment of Spent $LiFePO_4$ Batteries in China. *Resources, Conservation and Recycling* **2017**, *127*, 233–243. https://doi.org/10.1016/j.resconrec.2017.08.019.

(3) Xu, C.; Dai, Q.; Gaines, L.; Hu, M.; Tukker, A.; Steubing, B. Future Material Demand for Automotive Lithium-Based Batteries. *Commun Mater* **2020**, *1* (1), 99. https://doi.org/10.1038/s43246-020-00095-x.

(4) Kim, T.; Song, W.; Son, D.-Y.; Ono, L. K.; Qi, Y. Lithium-Ion Batteries: Outlook on Present, Future, and Hybridized Technologies. *J. Mater. Chem. A* **2019**, *7*(7), 2942–2964. https://doi.org/10.1039/C8TA10513H.

(5) Padhi, A. K.; Nanjundaswamy, K. S.; Goodenough, J. B. Phospho-olivines as Positive-Electrode Materials for Rechargeable Lithium Batteries. *J. Electrochem.*

Soc. **1997**, *144* (4), 1188–1194. https://doi.org/10.1149/1.1837571.

(6) Saw, L. H.; Somasundaram, K.; Ye, Y.; Tay, A. A. O. Electro-Thermal Analysis of Lithium Iron Phosphate Battery for Electric Vehicles. *Journal of Power Sources* **2014**, *249*, 231–238. https://doi.org/10.1016/j.jpowsour.2013.10.052.

(7) Wang, Y.; He, P.; Zhou, H. Olivine $LiFePO_4$: Development and Future. *Energy Environ. Sci.* **2011**, *4* (3), 805–817. https://doi.org/10.1039/C0EE00176G.

(8) Goodenough, J. B.; Kim, Y. Challenges for Rechargeable Li Batteries. *Chem. Mater.* **2010**, *22* (3), 587–603. https://doi.org/10.1021/cm901452z.

(9) Chen, C.; Ma, H.; Wang, Y. The Progress and Future Prospects of Lithium Iron Phosphate Cathode Materials. *HSET* **2022**, *3*, 31–42. https://doi.org/10.54097/hset.v3i.690.

(10) Xu, C.; Dai, Q.; Gaines, L.; Hu, M.; Tukker, A.; Steubing, B. Reply to: Concerns about Global Phosphorus Demand for Lithium-Iron-Phosphate Batteries in the Light Electric Vehicle Sector. *Commun Mater* **2022**, *3* (1), 15. https://doi.org/10.1038/s43246-022-00237-3.

(11) Li, H.; Xing, S.; Liu, Y.; Li, F.; Guo, H.; Kuang, G. Recovery of Lithium, Iron, and Phosphorus from Spent $LiFePO_4$ Batteries Using Stoichiometric Sulfuric Acid Leaching System. *ACS Sustainable Chem. Eng.* **2017**, *5* (9), 8017–8024. https://doi.org/10.1021/acssuschemeng.7b01594.

(12) Jialiang Zhang, Juntao Hu,Yubo Liu, Qiankun Jing, Cheng Yang, Yongqiang Chen,and Chengyan Wang. Sustainable and Facile Method for the Selective Recovery of Lithium from Cathode Scrap of Spent $LiFePO_4$ Batteries. *ACS Sustainable Chem. Eng.* **2019**, *7*, 5626–5631. https://doi.org/10.1021/acssuschemeng.9b00404.

(13) Kang, D.-K.; Shin, M.-Y.; Kim, D.-H.; Wang, J.-P. Selective Recovery of Lithium Sulfate from Spent LFP($LiFePO_4$) Powder. *IJETT* **2021**, *69* (11), 122–127. https://doi.org/10.14445/22315381/IJETT-V69I11P215.

(14) Cieślik, B.; Konieczka, P. A Review of Phosphorus Recovery Methods at Various Steps of Wastewater Treatment and Sewage Sludge Management. The Concept of "No Solid Waste Generation" and Analytical Methods. *J. Clean. Prod.* **2017**, *142*, 1728–1740. https://doi.org/10.1016/j.jclepro.2016.11.116.

(15) Kelessidis, A.; Stasinakis, A. S. Comparative Study of the Methods Used for Treatment and Final Disposal of Sewage Sludge in European Countries. *J. Waste Manag.* **2012**, *32* (6), 1186–1195. https://doi.org/10.1016/j.wasman.2012.01.012.

(16) Havukainen, J.; Nguyen, M. T.; Hermann, L.; Horttanainen, M.; Mikkilä, M.; Deviatkin, I.; Linnanen, L. Potential of Phosphorus Recovery from Sewage Sludge

and Manure Ash by Thermochemical Treatment. *J. Waste Manag.* **2016**, *49*, 221–229. https://doi.org/10.1016/j.wasman.2016.01.020.

(17) Donatello, S.; Tong, D.; Cheeseman, C. R. Production of Technical Grade Phosphoric Acid from Incinerator Sewage Sludge Ash (ISSA). *J. Waste Manag.* **2010**, *30* (8–9), 1634–1642. https://doi.org/10.1016/j.wasman.2010.04.009.

(18) Yu, H.; Lu, X.; Miki, T.; Matsubae, K.; Sasaki, Y.; Nagasaka, T. Sustainable Phosphorus Supply by Phosphorus Recovery from Steelmaking Slag: A Critical Review. *Resour., Conserv. Recycl.* **2022**, *180*, 106203. https://doi.org/10.1016/j.resconrec.2022.106203.

(19) Nakase K.; Matsui A.; Kikuchi N.; Miki Y. Effect of Slag Composition on Phosphorus Separation from Steelmaking Slag by Reduction. *Tetsu-to-Hagane* **2016**, *102* (9), 485–491. https://doi.org/10.2355/tetsutohagane.TETSU-2016-006.

(20) Koizumi, S.; Miki, T.; Nagasaka, T. Enrichment of Phosphorus Oxide in Steelmaking Slag by Utilizing Capillary Action. *J. Sustain. Metall.* **2016**, *2* (1), 38–43. https://doi.org/10.1007/s40831-015-0035-3.

(21) Iwama, T.; Du, C.; Koizumi, S.; Gao, X.; Ueda, S.; Kitamura, S. Extraction of Phosphorus and Recovery of Phosphate from Steelmaking Slag by Selective Leaching. *ISIJ Int.* **2020**, *60* (2), 400–407. https://doi.org/10.2355/isijinternational.ISIJINT-2019-298.

(22) Yu, H.; Miki, T.; Sasaki, Y.; Nagasaka, T. Simultaneous Reduction of P_2O_5 and FeO from CaO–SiO_2–FeO–P_2O_5 Synthesized Slag by Carbothermic Reduction. *Metall. Mater. Trans. B* **2022**, *53* (3), 1806–1815. https://doi.org/10.1007/s11663-022-02488-4.

(23) Yu, H.; Miki, T.; Sasaki, Y.; Nagasaka, T. Crystallography of the High-Temperature Ca_2SiO_4-$Ca_3P_2O_8$ Solid Solutions. *Metall. Mater. Trans. B* **2020**, *51* (6), 3007–3015. https://doi.org/10.1007/s11663-020-01945-2.

(24) Yu, Y.; Du, C. A Review on the P Enrichment and Recovery from Steelmaking Slag: Towards a Sustainable P Supply and Comprehensive Utilization of Industrial Solid Wastes. *Science of The Total Environment* **2023**, *891*, 164578. https://doi.org/10.1016/j.scitotenv.2023.164578.

(25) Du, C.-M.; Gao, X.; Ueda, S.; Kitamura, S.-Y. Separation and Recovery of Phosphorus from Steelmaking Slag via a Selective Leaching–Chemical Precipitation Process. *Hydrometallurgy* **2019**, *189*, 105109. https://doi.org/10.1016/j.hydromet.2019.105109.

(26) Mi, C. H.; Cao, G. S.; Zhao, X. B. Low-Cost, One-Step Process for Synthesis of Carbon-Coated $LiFePO_4$ Cathode. *Materials Letters* **2005**, *59* (1), 127–130.

https://doi.org/10.1016/j.matlet.2004.07.051.
(27) Yoshimi, I.; Shibayama, A.; Fujita, T.; Abe, K.; Miyazaki, T.; Sato, M.; Yen, W. T. Liberation of Materials by Electrical Disintegration for Recycling. *Int. J. Soc. Mater. Eng. Resour* 2002, *10* (1), 66–70.
https://doi.org/10.5188/ijsmer.10.66.